

RECENT QCD RESULTS IN $\nu - N$ DEEP-INELASTIC-SCATTERING AT CCFR/NUTEV

JAEOHOON YU

(for the CCFR/NuTeV Collaborations)
*MS309, FNAL, P.O.Box 500, Batavia,
 IL 60510, USA*
E-mail: yu@fnal.gov

We present recent QCD results in $\nu - N$ scattering at the Fermilab CCFR/NuTeV experiments. We present the latest Next-to-Next-Leading order strong coupling constant, α_s , extracted from Gross-Llewellyn-Smith sum rule. The value of α_s from this measurement, at the mass of Z boson, is $\alpha_s^{NNLO}(M_Z^2) = 0.114^{+0.009}_{-0.012}$. We also present a preliminary result of the CCFR F_2 at large- x . This measurement of F_2 is compared to other experiments and various models that provide nuclear effects. We discuss the previous strange sea quark measurement from the CCFR experiment and the prospects for improvements of the measurement in the NuTeV experiment.

1 Introduction

Neutrino-nucleon (ν -N) deep inelastic scattering (DIS) experiments provide a good testing field for Quantum Chromo-Dynamics (QCD), the theory of strong interactions. The ν -N DIS experiments probe the structure of nucleons and provide an opportunity to test QCD evolutions and to extract the strong coupling constant, α_s . They are complementary measurements to charged lepton DIS experiments of nucleon structure functions. The advantage of ν -N DIS measurements over the charged lepton experiments is that ν -N experiments can measure both $F_2(x, Q^2)$ and $xF_3(x, Q^2)$ due to pure V-A nature. The $\nu - N$ differential cross sections are written, in terms of structure functions:

$$\frac{d^2\sigma^{\nu(\bar{\nu})}}{dxdy} = \frac{G_F^2 ME_\nu}{\pi} \left[\left(1 - y - \frac{Mxy}{2E_\nu} + \frac{y^2}{2} \frac{1 + 4M^2x^2/Q^2}{1 + R(x, Q^2)} \right) F_2^{\nu(\bar{\nu})} \right. \\ \left. \pm \left(y - \frac{y^2}{2} \right) xF_3^{\nu(\bar{\nu})} \right] \quad (1)$$

where $R(x, Q^2) = \sigma_L/\sigma_T$, the ratio of longitudinal to transverse absorption cross sections. The structure functions $F_2(x, Q^2)$ and $xF_3(x, Q^2)$ are extracted from fitting Eq. 1 to the measured differential cross sections.

In this paper, we present a next-to-next leading order (NNLO) determination of α_s from the Gross-Llewellyn-Smith (GLS) sum rule and a large- x structure function measurement from the CCFR experiment. We also discuss

the measurements of strange sea quark distributions from the CCFR experiment and the expected improvements of this measurement in NuTeV.

2 The Experiments

CCFR (Columbia-Chicago-Fermilab-Rochester)/NuTeV experiment is a $\nu - N$ DIS experiment at the Tevatron in Fermilab. The CCFR experiment used a broad momentum beam of mixed neutrinos (ν_μ) and antineutrinos ($\bar{\nu}_\mu$) from decays of the secondary pions and kaons, resulting from interactions of 800GeV primary protons on a Beryllium-Oxide (BeO) target. The NuTeV experiment, the successor of CCFR, used separate beams of ν_μ or $\bar{\nu}_\mu$ during a given running period, using a Sign-Selected-Quadrupole-Train (SSQT) ¹.

The CCFR/NuTeV detector ² consists of two major components : target calorimeter and muon spectrometer. The target calorimeter is an iron-liquid-scintillator sampling calorimeter, interspersed with drift chambers to provide track information of the muons resulting from charged-current (CC) interactions where a charged weak boson (W^+ or W^-) is exchanged between the ν_μ ($\bar{\nu}_\mu$) and the parton. The calorimeter provides dense material in the path of ν ($\bar{\nu}$) to increase the rate of neutrino interactions. The hadron energy resolution of the calorimeter is measured from the test beam and is found to be : $\sigma/E_{Had} = (0.847 \pm 0.015)/\sqrt{E_{Had}(GeV)} + (0.30 \pm 0.12)/E_{Had}$.

The muon spectrometer is located immediately downstream of the target calorimeter and consists of three toroidal magnets and five drift chamber stations to provide accurate measurements of muon momenta. The momentum resolution of the spectrometer (σ/p_μ) is approximately 10.1% and the angular resolution is $\theta_\mu = 0.3 + 60/p_\mu$ (mrad).

3 α_s from Gross-Llewellyn-Smith Sum Rule

Once the structure function xF_3 is extracted, one can use the Gross-Llewellyn-Smith (GLS) sum rule ³, which states that $\int xF_3(dx/x)$ is the total number of valence quarks in a nucleon, up to QCD corrections, to extract the strong coupling constant, α_s . Since in leading order (LO), the structure function xF_3 is $xq - x\bar{q}$, the valence quark distributions, integrating xF_3 over x yields total number of valence quarks, 3.

Since the GLS sum rule is a fundamental prediction of QCD and the integral only depends on valence quark distributions, α_s can be determined without being affected by less well known gluon distributions. Moreover, since there are sufficient number of measurements of xF_3 in a wide range of Q^2 , one can measure α_s as a function of Q^2 in low Q^2 where the values of α_s depends most on Λ_{QCD} .

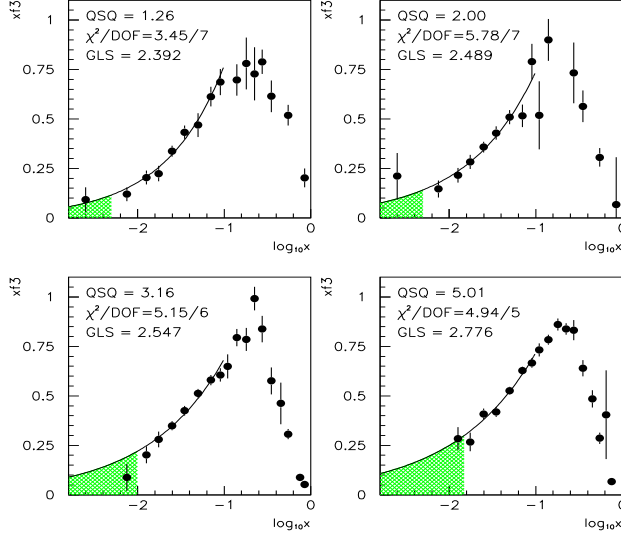


Figure 1: xF_3 vs x for four lowest Q^2 bins. The solid circles represent the CCFR xF_3 data and the inverse triangle represent the data from other experimental measurements.

With next-to-next-to-leading order QCD corrections⁴, the GLS integral takes the form :

$$\int_0^1 xF_3(x, Q^2) \frac{dx}{x} = 3 \left(1 - \frac{\alpha_s}{\pi} - a(n_f) \left(\frac{\alpha_s}{\pi} \right)^2 - b(n_f) \left(\frac{\alpha_s}{\pi} \right)^3 \right) - \Delta HT \quad (2)$$

where the term ΔHT is the corrections from higher-twist effects. The higher-twist correction term, ΔHT , is predicted to be significant in some models⁵, while others⁶ predict negligibly small corrections. We take ΔHT as one half the largest model prediction with the associated error covering the full range ($\Delta HT = (0.15 \pm 0.15)/Q^2$).

In order to perform the integration of xF_3 in the entire ranges of x , we use data from other ν -N DIS experiments (WA59, WA25, SKAT, FNAL-E180, and BEBC-Gargamelle⁷), to cover large- x ranges that are not covered by CCFR due to geometric and kinematic acceptances. The CCFR data has a minimum x of roughly $x = 0.002Q^2$. To extrapolate below this kinematic limit, we fit xF_3 to a power law (Ax^B) using all the data points in $x < 0.1$.

Since the data points do not populate the region $x > 0.5$ finely, it is necessary to interpolate between the data points. Thus, we use the shapes of

the charged lepton DIS F_2 in $x > 0.5$, because the shapes of xF_3 and F_2 should be the same in this region of x due to negligible contribution from sea quarks. The charged lepton F_2 data are corrected for nuclear effects⁸ before obtaining the shapes. Systematic uncertainties due to extrapolation and interpolation take into account the possible variations of the models in the low- x region and the resonance peaks in charged-lepton F_2 shapes in large- x regions.

Figure 1 shows xF_3 in the four lowest Q^2 bins as a function of x . The solid circles represent the experimental xF_3 data, The solid lines represent the power law fit used for extrapolation of xF_3 outside the kinematic limit of CCFR. The shaded area in each plot shows the region of x where the extrapolations are used for the integration.

The xF_3 integrals are estimated in six Q^2 bins. The results in each Q^2 bin are fit to the NNLO pQCD function and higher-twist effect in Eq. 2. This procedure yields a best fit of $\Lambda_{\overline{MS}}^{5,NNLO} = 165\text{MeV}$. Evolving this result to the mass of the Z boson, M_Z , in NNLO, this corresponds to the value of α_s :

$$\alpha_s^{NNLO}(M_Z^2) = 0.114^{+0.005}_{-0.006}(\text{stat.})^{+0.007}_{-0.009}(\text{syst.}) \pm 0.005(\text{theory}) \quad (3)$$

where systematic uncertainty includes the error in the fit and theory error represents the uncertainty due to higher twist effects and higher order QCD contributions. This result is consistent with the value extracted from the CCFR structure function measurement⁹.

Evolving to the mean value of Q^2 ($= 3\text{GeV}^2$) for this analysis results in $\alpha_s^{NNLO}(3\text{GeV}^2) = 0.278 \pm 0.035 \pm 0.05^{+0.035}_{-0.03}$. If the higher-twist effect is neglected, the value of $\alpha_s^{NNLO}(M_Z^2)$ becomes 0.118.

4 Large- x Structure Functions

In a simple parton model, the contributions of a single stationary nucleons vanish as x , the fractional parton momentum, approaches to 1. However, the interplays between nucleons in a nuclear environment would add a momentum to initial nucleon that interacts with the neutrino, causing x to be greater than 1. This nuclear effect has been observed and measured in EMC experiment and is called the EMC effect⁸.

There have been several models to describe this nuclear effect : 1) Fermi-gas model which adds Fermi momentum¹⁰ and a quasi-deuteron effect¹¹, 2) few nucleon correlation model¹² and 3) the multi-quark cluster model¹³, which add exponentially falling F_2 distributions.

In order to explore these various models, the CCFR experiment measured large- x cross sections in the kinematic regions $x > 0.75$ and $Q^2 > 50\text{GeV}^2$. This measured cross section is compared to a LO Monte Carlo predictions

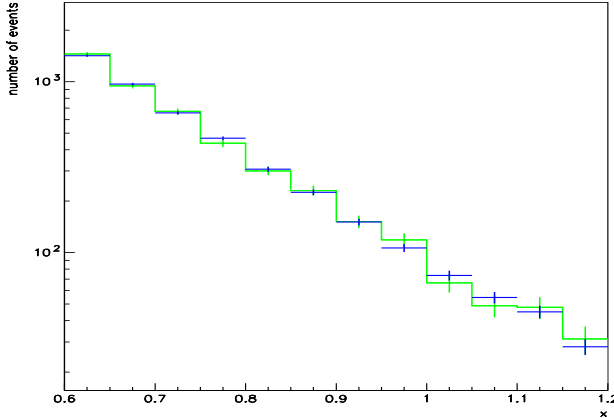


Figure 2: Number of events vs x for all events in $Q^2 > 50\text{GeV}^2$. The histogram represent the data and the points represents the fit results.

that includes various detector smearing effects and incorporates various models separately. Figure 2 shows the number of events as a function of the scaling variable x in the region $x > 0.75$. The structure function $F_2(x, Q^2)$ is then fit to the functional form ¹⁴ $F_2(x, Q^2) = (1 - x)^a(b + cx + dx^2 + ex^3)(Q^2)^{f+gx}$ ^a for $x < 0.75$ and $F_2(x, Q^2) = F_2(x = 0.75, Q^2)e^{-s(x-0.75)}$ for $x > 0.75$. The resulting value of the parameter s from this fit is $s = 8.3 \pm 0.7(\text{stat}) \pm 0.3(\text{syst})$.

We also investigated a possible Q^2 dependence of this parameter s in two Q^2 bins, $50 < Q^2 < 100 \text{ GeV}^2$ and $100 < Q^2 < 400 \text{ GeV}^2$. The resulting values of the parameter s in these two kinematic regions are $s = 7.4 \pm 0.9$ for lower Q^2 bin and $s = 8.7 \pm 0.9$ in the higher Q^2 bin, showing only a weak Q^2 dependences. Table 1 compares this result with other experimental measurements and models, demonstrating that the FNC prediction and the SLAC E133 measurement of the parameter s agree with our result, while the

Table 1: Comparisons of the exponent s of CCFR with other predictions and experimental measurements.

Experiment/Predictions	s
CCFR	8.3 ± 0.8
FNC Prediction	$8 \sim 9$
Baldin <i>et al.</i> Prediction	~ 6
SLAC E133	$7 \sim 8$
BCDMS	16.5 ± 0.5

^aa:2.5693, b=0.2739, c=3.0437, d=-5.5172, e=2.5790, f=-0.0303, and g=-0.2185

BCDMS result differs significantly.

From this analysis, we find that the models without nuclear effect do not describe our data well. Incorporating only Fermi gas and quasi-deuteron model is not enough to describe the excess of the data over $x > 1$. The FNC model describes the CCFR large- x behavior well with the exponential fall off parameter of $s = 8.3 \pm 0.9$. This measurement indicates that the nucleon structure function F_2 at $x = 1$ does not vanish but has a finite value¹⁵ of $\sim 2 \times 10^{-3}$.

5 Strange Sea Measurements

In $\nu - N$ DIS, the flavor changing weak CC interactions provide a clean signature for a scattering off an s quark ($s \rightarrow c$), resulting in a pair of oppositely signed muons in the final state through the reaction $\nu_\mu(\bar{\nu}_\mu) + N \rightarrow \mu^-(\mu^+) + c(\bar{c}) + X$ where $c(\bar{c})$ subsequently undergoes a semileptonic decay $c(\bar{c}) \rightarrow s(\bar{s}) + \mu^+(\mu^-) + \bar{\nu}_\mu(\nu_\mu)$. In contrast, detecting s quark with NC interactions in a charged lepton DIS is convoluted with s production and fragmentation of strange mesons, requiring good particle identifications. The nucleon structure function F_2 from $\nu - N$ DIS together with that measured from charged lepton DIS could also measure s quark distributions. In addition, the difference of the $\nu - N$ structure function xF_3 between ν and $\bar{\nu}$ measures the nucleon strange quark contents as well.

CCFR experiment performed both LO¹⁶ and NLO analyses¹⁷. Since a neutrino from the semileptonic decay of the charm is involved in the final state, the CCFR measured the distributions of visible physical quantities; x_{vis} , $E_{vis} = E_{Had} + p_\mu^1 + p + \mu^2$, and $z_{vis} = \frac{p_\mu^2}{E_{Had} + p_\mu^2}$ which is the fractional momentum taken by the charm meson fragmentation. The measured distributions were compared to Monte Carlo predictions which incorporate detector acceptance and resolutions.

The Monte Carlo included the singlet ($xq_{S1}(x, \mu^2)$), non-singlet ($xq_{NS}(x, \mu^2) = xq_V(x, \mu^2)$), and gluon parton distribution functions from CCFR structure function analysis assuming:

$$xq_V(x, \mu^2) = xu_V(x, \mu^2) + xd_V(x, \mu^2) \quad (4)$$

$$xd_V(x, \mu^2) = A_d(1 - x)xu_V(x, \mu^2) \quad (5)$$

$$x\bar{u}(x, \mu^2) = xu_S(x, \mu^2) \quad (6)$$

$$x\bar{d}(x, \mu^2) = xd_S(x, \mu^2) \quad (7)$$

The above assumes symmetric sea quark distributions. We then parameterized

the strange sea distribution to:

$$xs(x, \mu^2) = A_s(1 - x)^\alpha \left[\frac{x\bar{u}(x, \mu^2) + x\bar{d}(x, \mu^2)}{2} \right] \quad (8)$$

where, A_s is defined in terms of level and shape parameters, κ and α . The level parameter κ is defined as :

$$\kappa = \frac{\int_0^1 [xs(x, \mu^2) + x\bar{s}(x, \mu^2)]}{\int_0^1 [x\bar{u}(x, \mu^2) + x\bar{d}(x, \mu^2)]} \quad (9)$$

The LO prediction included a simple parton model which has tree level calculations for scattering of a W off an s quark, resulting in a charm quark final state. On the other hand, the NLO prediction included the ACOT formalism¹⁸ whose calculation is performed in a variable flavor $\overline{\text{MS}}$ scheme. Specifically the NLO prediction included the Born and gluon-fusion diagrams. In addition, since the charm quark is massive, the threshold effect was taken into account in the prediction via leading order slow rescaling formalism where the scaling variable x is replaced with ξ defined as :

$$\xi = x \left(1 + \frac{m_c^2}{Q^2} \right) \left(1 - \frac{x^2 M^2}{Q^2} \right), \quad (10)$$

where m_c is the mass of the charm quark.

We then fit the Monte Carlo to data distributions of x_{vis} , E_{vis} , and z_{vis} for κ , α , B_c (the charmed meson semi-leptonic branching ratio), m_c , and ϵ (fragmentation parameter), using the values of CKM matrix elements $|V_{cd}|$ and $|V_{cs}|$, taken from PDG¹⁹.

Table 2 summarizes the results of this analysis, comparing various fragmentation functions at LO and NLO. The result shows that the strange sea level parameter, κ , is in qualitative agreement between LO and NLO analyses while the shape parameter, α , is the same as other sea quarks in NLO but softer in LO. The charm quark mass differs between NLO and LO, due presumably to the fact that the parameter m_c is not a pole mass but rather a theoretical parameter that absorbs the lack of higher corrections.

Aside from the large statistical uncertainty, there were two major sources of systematic uncertainties in performing this measurement in CCFR. First and foremost one is the identification of the secondary muons resulting from the decay of charmed mesons. Since the neutrino beam in CCFR was a mixture of ν_μ and $\bar{\nu}_\mu$, the experiment relied on transverse momentum of the muons relative to the neutrino beam direction, P_T^μ , to distinguish the prompt muons from

Table 2: Summary of the CCFR strange sea analysis. The first set of the errors in each item is statistical and the second set is the systematic uncertainties.

	Fragmentation	κ	α	B_c	$m_c(\text{GeV})$
NLO	Collins-Spiller	0.477	-0.02	0.1091	1.70
	$\epsilon = 0.81$	+0.046 -0.044 ±0.14	+0.60 -0.54 +0.28 -0.26	+0.0082 -0.0074 +0.0063 -0.0051	±0.17 +0.09 -0.08
	Peterson	0.468	-0.05	0.1047	1.69
NLO	$\epsilon = 0.20$	+0.061 -0.046 ±0.04	+0.46 -0.47 +0.28 -0.26	±0.0076 +0.0065 -0.0052	±0.16 +0.12 -0.10
	Peterson	0.373	2.50	0.1050	1.31
	$\epsilon = 0.20$	+0.048 -0.041 ±0.04	+0.60 -0.55 +0.36 -0.25	±0.007 +0.005	+0.20 -0.22 +0.12 -0.11
LO					

secondary muons. The second systematic uncertainty is the LO slow rescaling formalism to take into account the charm threshold effect in theoretical predictions.

The experimental systematic uncertainty due to the identification of the secondary muon almost completely disappears in the NuTeV experiment due to the use of SSQT whose wrong sign neutrino contamination at a given mode is less than 10^{-3} . In addition, the NuTeV experiment is working on improving low energy muon energy measurements in the calorimeter using the intensive calibration beam program. In the theoretical predictions, NuTeV is planning to incorporate more complete NLO calculations and will investigate the dependence of the predictions on factorization scheme and various parton distribution function parameterizations.

While statistical uncertainty dominated in the previous measurement, improving the systematic uncertainty would reduce the total error significantly. We expect the statistical uncertainty in this analysis would reduce by about a factor of 2.2 combining CCFR and NuTeV data. The NuTeV is currently planning to present a LO analysis by this summer.

6 Conclusions

CCFR measured GLS integral in six Q^2 bins and extracted the value of NNLO α_s at the mass of the Z boson. The measured value of α_s is:

$$\alpha_s^{NNLO}(M_Z^2) = 1.114^{+0.009}_{-0.012} \quad (11)$$

which is consistent with the value measured from the structure function analysis⁹ and with world average. CCFR measured the large- x cross sections in

the region $x > 0.75$. Comparisons with various nuclear model seems to point that the FNC model along with Fermi-gas and quasi-deuteron model describe the data well with the exponential fall off parameter $s = 8.3 \pm 0.9$. The value of F_2 at $x = 1$ is measured to be $F_2^{\nu Fe}(x = 1) = 2.1 \times 10^{-3}$.

NuTeV has finished data taking in September 1997, running with separate beams of ν_μ and $\bar{\nu}_\mu$, and a precision calibration (0.3%) is underway. Strange sea measurement at the NuTeV experiment is making progress, taking advantage of the separate beam and the intensive calibration. NuTeV expects a LO result in the strange sea measurement by the summer.

References

1. R.H.Bernstein *et al.*, NuTeV Collaboration, “Technical Memorandum:Sign Selected Quadrupole Train,” FERMILAB-TM-1884 (1994); J.Yu *et al.*, NuTeV Collaboration, “Technical Memorandum : NuTeV SSQT performance,” FERMILAB-TM-2040 (1998).
2. W.K.Sakumoto *et al.*, CCFR Collaboration, Nucl. Instr. Meth. **A294**, 179 (1990).
3. D.J.Gross & C.H.Llewellyn Smith, *Nucl. Phys.* **B14**, 337 (1969).
4. S.A.Larin & J.A.M.Vermarseren, *Phys. Lett.* **B274**, 221 (1991).
5. V.M.Braun & A.V.Kolesnichenko, *Nucl. Phys* **B283**, 723 (1987).
6. S.Fajner and R.J. Oakes, *Phys. Lett.* **B163**, 385 (1985); M.Dasgupta and B.R. Webber, *Phys. Lett.* **B382**,273 (1996); U.K. Yang, A. Bodek, and Q. Fang, in these proceedings
7. K.Varvell *et al.*, *Z. Phys.* **C36**, 1 (1987) D.Allasia *et al.*, *Z. Phys.* **C28**, 321 (1985); V.V.Ammosov *et al.*, *Z. Phys.* **C30**, 175 (1986); V.V.Ammosov *et al.*, *JETP* **36**, 300 (1982); P.C. Bosetti *et al.*, *Nucl. Phys.* **B142**, 1 (1978).
8. D.F. Geesaman, K. Saito, and A.W. Thomas, *Ann. Rev. Part. Sci.* **45**, 337 (1995).
9. W.Seligman *et al.*, CCFR/NuTeV Collaboration, *Phys. Rev. Lett.* **79**, 1213 (1997).
10. E.J.Monitz, *Phys. Rev.* **26**, 445 (1971).
11. A. Bodek and J.L. Ritchie, *Phys. Rev.* **D24**, 1200 (1981).
12. L.Frankfurt and M. Strikman, *Phys. Rep.* **76**, 215 (1981).
13. L.A.Kondratyuk and M.Zh.Shmatikov, *Yad. Fiz.* **41**, 222 (1985).
14. BCDMS Collaboration, *Z. Phys.* **C63**, 29 (1994).
15. M.Vakili, Thesis, University of Cincinnati, August, Unpublished (1997).
16. S.A. Rabinowitz *et al.*, CCFR Collaboration, *Phys. Rev. Lett.* **70**, 134 (1993).

17. A.O.Bazako *et al.*, CCFR Collaboration, Z. Phys. **C65**, 189 (1995).
18. M.A.G. Avaziz, J.C.Collins, F.I. Olness, and W.K.Tung, Phys. Rev. **D50**, 3102 (1994).
19. Particle Data Group, Phys. Rev. **D45** (1990).